JOURNAL OF BACTERIOLOGY, Nov. 2011, p. 5936–5949 Vol. 193, No. 21
0021-9193/11/$12.00 doi:10.1128/JB.05877-11

Expression during Host Infection and Localization of *Yersinia pestis* Autotransporter Proteins▽

Jonathan D. Lenz,[1,3,4] Matthew B. Lawrenz,[1,4]† David G. Cotter,[4] M. Chelsea Lane,[1] Rodrigo J. Gonzalez,[2] Michelle Palacios,[2] and Virginia L. Miller[1,2,3,4]*

Department of Genetics, University of North Carolina, Chapel Hill, North Carolina[1]; Department of Microbiology and Immunology, University of North Carolina, Chapel Hill, North Carolina[2]; Division of Biology and Biomedical Sciences, Washington University, Saint Louis, Missouri 63110[3]; and Department of Molecular Microbiology, Washington University, Saint Louis, Missouri 63110[4]

Received 25 July 2011/Accepted 17 August 2011

***Yersinia pestis* CO92 has 12 open reading frames encoding putative conventional autotransporters (*yaps*), nine of which appear to produce functional proteins. Here, we demonstrate the ability of the Yap proteins to localize to the cell surface of both *Escherichia coli* and *Yersinia pestis* and show that a subset of these proteins undergoes processing by bacterial surface omptins to be released into the supernatant. Numerous autotransporters have been implicated in pathogenesis, suggesting a role for the Yaps as virulence factors in *Y. pestis*. Using the C57BL/6 mouse models of bubonic and pneumonic plague, we determined that all of these genes are transcribed in the lymph nodes during bubonic infection and in the lungs during pneumonic infection, suggesting a role for the Yaps during mammalian infection. *In vitro* transcription studies did not identify a particular environmental stimulus responsible for transcriptional induction. The primary sequences of the Yaps reveal little similarity to any characterized autotransporters; however, two of the genes are present in operons, suggesting that the proteins encoded in these operons may function together. Further work aims to elucidate the specific functions of the Yaps and clarify the contributions of these proteins to *Y. pestis* pathogenesis.**

Yersinia pestis is a vector-borne pathogen that primarily infects wild rodents, where the transmission cycle is maintained by passage through a flea vector (21, 39). Humans can become incidental hosts for this bacterium when they come into contact with infected fleas, animals, or contaminated environments (20, 22, 54). *Y. pestis* is able to rapidly disseminate from the site of inoculation (typically a flea bite) to the regional lymph nodes, where it multiplies to high numbers, causing a painful lymph node inflammation (a bubo) that is the hallmark symptom of bubonic plague. Without treatment, the bacteria can enter the circulatory system and achieve a high titer in the blood, causing severe disease in the host and allowing for efficient continuation of the vector-borne transmission cycle (46). Colonization of the lungs and development of secondary pneumonic plague can result in person-to-person transmission via inhalation of aerosolized droplets contaminated with *Y. pestis*. Both septicemic and pneumonic plague are associated with high rates of mortality. Though widely known as the cause of three historic pandemics (54), epidemics and epizootics of *Y. pestis* are still regular occurrences in areas where this organism is endemic in wild rodent populations (17, 49). Factors such as climatic variability and the mobility of human populations have contributed to the reemergence of this pathogen (6, 10).

* Corresponding author. Mailing address: 116 Manning Drive, CB 7290, University of North Carolina, Chapel Hill, NC 27599. Phone: (919) 966-9956. Fax: (919) 962-8103. E-mail: vlmiller@med.unc.edu.

† Present address: Center for Predictive Medicine for Biodefense and Emerging Infectious Diseases, Department of Microbiology and Immunology, University of Louisville Medical School, Louisville, KY.

▽ Published ahead of print on 26 August 2011.

Y. pestis recently evolved into a vector-borne pathogen from the food-borne pathogen *Yersinia pseudotuberculosis* (1). During this adaptation, it lost virulence factors through mutations that are specific for an enteric life style (34, 51) and acquired virulence factors specific to *Y. pestis*. This is evident by the high number of pseudogenes in the *Y. pestis* genome and is highlighted by mutations in the genes *inv* and *yadA*. Inv and YadA are the primary adhesins of *Y. pseudotuberculosis* and *Yersinia enterocolitica* and have been shown to be important for gastrointestinal colonization (36, 52, 62). Furthermore, both proteins have been implicated in mediating interactions with eukaryotic cells that lead to efficient translocation of the Yop effector proteins into host cells through a type III secretion system (23, 56). It is likely that other *Y. pestis* pseudogenes are also important for fecal-oral transmission and that *Y. pestis* currently is accumulating additional mutations in other genes that do not provide a selective advantage during plague infection (14, 70).

Gram-negative bacteria have evolved at least six major secretion pathways to export proteins across their inner and outer membranes (types I to VI). The type V secretion pathway is perhaps the simplest. Type V proteins have a conserved structure that includes three distinct domains that provide information necessary to mediate secretion, a property that originally led members of this family to be referred to as autotransporters. For these proteins to be secreted, an amino-terminal signal peptide first targets the autotransporter to the general secretory apparatus for secretion across the inner membrane. Once in the periplasm, recent studies suggest that many autotransporters interact with conserved periplasmic chaperones and the Bam (Omp85) complex to stabilize the unfolded passenger domain and properly insert the β-domain into the outer membrane (11, 40, 57–59). Translocation of the

passenger domain from the periplasm across the outer membrane results in surface exposure of the mature passenger domain, where in some cases it is further processed and released. While the signal peptide and β-domain are highly conserved in autotransporters, the passenger domains vary greatly between different proteins and have been shown to perform a wide variety of functions. Many of these functions contribute to pathogenesis and include adherence to eukaryotic cells, cytotoxicity, proteolysis, and complement resistance (9).

Initial annotation of *Y. pestis* sequenced genomes resulted in the identification of several open reading frames (ORFs) that contained putative β-domains. Those genes possessing β-domains share a phylogenetic relationship with other conventional autotransporters (16) and have been referred to as Yaps, for *Yersinia* autotransporter proteins. In *Y. pestis* CO92 (biovar Orientalis), seven *yap* genes were initially annotated (*yapA*, *yapB*, *yapC*, *yapE*, *yapF*, *yapG*, and *yapH*) and given the designation of putative autotransporter proteins. In the genome of *Y. pestis* KIM (biovar Medievalis), Yen et al. identified 10 open reading frames that contained putative β-domains and their studies in *Escherichia coli* suggested that at least five of these proteins localize to the outer membrane (72). Additional studies have since indicated that a subset of these putative autotransporter proteins possesses adhesive and autoaggregative properties (24, 42, 72). As more investigation has been initiated into the virulence properties of *Y. pestis*, some of these putative autotransporter-encoding genes have arisen in genetic screens as having potential roles in host infection or encoding immunogenic proteins (4, 27, 43, 71) though their contributions to pathogenesis remain largely undefined.

The role of autotransporters as virulence factors in other bacteria suggests that the *Yersinia* autotransporters contribute to the virulence of *Y. pestis*. As a first step toward gaining an understanding of the function of the Yaps and their potential role in virulence, we investigated their localization and expression patterns. To determine if the Yaps do indeed localize in a manner predicted by bioinformatics analyses, we examined the localization of Yaps expressed in *E. coli* and in *Y. pestis*. In addition, the transcriptional profile of the *yap* genes during mammalian infection and in response to exposure to several potential environmental signals was assessed.

MATERIALS AND METHODS

***In silico* identification of putative autotransporters.** To identify putative conventional autotransporters in *Yersinia*, we initially searched the Pfam protein database for *Y. pestis* proteins containing predicted β-domains (PF03797) (25). Additional putative autotransporters in *Y. pestis* CO92 and all the putative autotransporters in *Y. pseudotuberculosis* and *Y. enterocolitica* were identified through BLAST analysis using the previously identified *Y. pestis* CO92 β-domain sequences identified in Pfam (3, 26) and from the characterized autotransporters TibA and AIDA-1. The location of β-domains was predicted through sequence analysis using Pfam, and signal peptide prediction was accomplished with SignalP, version 3.0 (8).

Bacterial strains and growth conditions. All bacterial strains and plasmids used in this study are listed in Table 1. *Y. pestis* CO92 was cultivated on brain heart infusion (BHI) agar (BD Biosciences, Bedford, MA) at 26°C for 48 h and in liquid cultures grown in BHI broth with aeration at 26°C or 37°C as indicated. *E. coli* strains were cultivated on Luria-Bertani (LB) agar (BD Biosciences) at 37°C overnight and in liquid cultures grown in LB medium at 37°C with aeration. When appropriate, antibiotics were used at the following concentrations: kanamycin, 50 μg ml^{-1}; carbenicillin, 50 μg ml^{-1}; and spectinomycin, 100 μg ml^{-1}.

For transcription analysis, saturated overnight cultures of *Y. pestis* CO92 pCD1$^-$ (YP6) were grown at 26°C and diluted to an initial optical density at 600 nm (OD_{600}) of 0.2 followed by growth, with aeration, at 26°C or 37°C to an OD_{600} of 1.0 to 1.8 (3 to 4 h). A total of 1×10^9 cells were harvested from these cultures for RNA extraction. For analysis of the impact of exogenous calcium on gene expression, cultures were supplemented with 2.5 mM $CaCl_2$. The impact of iron limitation was assessed in cultures grown as indicated above for 3 h and then supplemented with the iron chelator 2,2′-dipyridyl (Sigma, St. Louis, MO) to a final concentration of 100 μM for one additional hour of growth. To determine the impact of pH on growth, BHI medium was buffered with 100 mM MES [2-(*N*-morpholino)ethansulfonic acid] (Sigma) and then adjusted to pH 6.0, buffered with 100 mM PIPES [piperazine-*N*,*N*′-*bis*(2-ethansulfonic acid)] (Sigma) and then adjusted to pH 7.0, or buffered with 100 mM TAPS [*N*-tris(hydroxymethyl)methyl-3-aminopropanesulfonic acid] (Sigma) and then adjusted to pH 8.0. For immunofluorescence studies, *Y. pestis* CO92 pCD1$^-$ strains carrying pMWO-005-based vectors were cultured as for transcription analysis, with the exception of the addition of 50 μg ml^{-1} kanamycin to all cultures.

Plasmid and strain construction. In order to generate hemagglutinin (HA) epitope-tagged *yap* genes, we modified the pLP-PROTet-6xHN plasmid (Clontech, Mountain View, CA) to include the *yadA* signal sequence in frame with an HA tag, followed by XmaI/SmaI, NheI, and BglII restriction sites. The *yadA* signal sequence was amplified by PCR with the primers pSS fwd and pSS rev. The primer pSS fwd includes an EcoRI site and a ribosome binding site upstream of the *yadA* signal sequence. The primer pSS rev includes the XmaI/SmaI, NheI, BglII, and HindIII restriction sites. The PCR product and pLP-PROTet-6xHN plasmid were digested with EcoRI and HindIII and ligated to generate pSS. Each of the *yap* genes was amplified by PCR with gene-specific primers (Table 2) from *Y. pestis* CO92 genomic DNA; primers were designed to amplify each full-length gene without the predicted signal sequence (Table 2). PCR products and pSS were digested with either XmaI, SmaI, or NheI and HindIII and then ligated to generate plasmids with each *yap* oriented in frame with a start codon, *yadA* signal sequence, and HA tag. For expression of tagged proteins, pSS-based plasmids were transformed by electroporation into *E. coli* DH5αPRO (Clontech) or UT5600 (Δ*ompT*) containing pVM1286, which harbors the tetracycline repressor (Clontech). To allow for the production of HA-tagged *yap* genes in *Y. pestis*, the previously constructed pSS plasmids were digested with either BssSI and HindIII (*yapE*, *yapG*, *yapJ*, *yapK*, and *yapM*), BssSI and BamHI (*yapA*), or BbsI and HindIII (*yapF* and *yapL*) to produce a fragment with all relevant inducible promoter/operator elements followed by the full-length HA-tagged gene. These fragments were ligated into similarly digested pMWO-005, a low-copy-number vector carrying origins compatible with both *Y. pestis* and *E. coli* (M. W. Obrist and V. L. Miller, unpublished data), and transformed by electroporation into DH5α as above. Completed plasmids were isolated and transformed into *Y. pestis* CO92 pCD1$^-$.

Surface proteolysis and Western blot analysis. Surface proteolysis, supernatant precipitation, and SDS-PAGE were performed as described previously for the *Yersinia* autotransporter protein YapE (42) with the exception that 20 ng ml^{-1} of anhydrous tetracycline (aTc) (Sigma) was used for protein induction in *E. coli* DH5αPRO backgrounds, and 100 ng ml^{-1} was used in *E. coli* UT5600 and *Y. pestis* backgrounds. For Western analysis, monoclonal anti-HA mouse serum (Sigma) and anti-maltose-binding protein (MalE) rabbit serum (New England BioLabs, Ipswich, MA) were used at a concentration of 1:10,000. Peroxidase-conjugated secondary antibodies were used at a concentration of 1:50,000.

Immunofluorescence microscopy. For immunofluorescence, protease-treated and untreated samples were suspended in 1 ml of phosphate-buffered saline (PBS), and 10 μl was removed to a poly-D-lysine-coated coverslip (BD Biosciences) and allowed to dry. The remainder of each sample was retained for analysis by SDS-PAGE. Bacteria were fixed on coverslips with 4% paraformaldehyde and washed four times with PBS prior to incubation with a 1:500 dilution of Alexa Fluor 488-conjugated monoclonal mouse anti-hemagglutinin IgG (Life Technologies, Carlsbad, CA) prepared in 2% goat serum (Life Technologies). Slides were washed three times with PBS, dried, and mounted with Prolong Gold reagent (Life Technologies) prior to imaging on an Olympus BX61 fluorescence microscope. At least three fields were selected for each sample, and paired differential interference contrast (DIC) and fluorescein isothiocyanate (FITC) images were obtained for each field. Exposures were set for positive-control samples and held constant when imaging protease-treated samples to accurately represent the presence or absence of fluorescent signal. Images were obtained digitally using a Hamamatsu ORCA RC camera and Volocity imaging software (PerkinElmer, Waltham, MA). Images were prepared for presentation using Photoshop and Illustrator CS5 (Adobe Systems).

Animal infections and tissue collection. All animal experiments were approved by the University of North Carolina Institutional Animal Care and Use Committee (protocol 08-144.0). Four- to 6-week-old female C57BL/6J mice (Jackson Laboratory, Bar Harbor, ME) were allowed free access to sterilized food and

TABLE 1. Bacterial strains and plasmids used in this study

Strain or plasmid	Description[a]	Reference or source
E. coli strains		
DH5αPRO	*deoR endA1 gyrA96 hsdR17*(r_K^- m_K^+) *recA1 relA1 supE44 thi-1* Δ(*lacZYA-argF*)*U169* ϕ80d*lacZ*ΔM15 F^- λ^- P_{N25} *tetR* P_{lacI}^q *lacI* Sp^r	Clontech
S17-1λ*pir*	Tp^r Str^r *recA thi pro hsdR hsdM* $^+$ RP4::2-Tc::Mu::Km Tn*7* λ*pir* lysogen	50
UT5600	F^- *ara-14 leuB6 secA6 lacY1 proC14 tsx-67* Δ(*ompT-fepC*)*266 entA403 trpE38 rfbD1 rpsL109 xyl-5 mtl-1 thi-1*	New England Biolabs
Y. pestis strains		
YP4	CO92, polymyxin B resistant	20
YP6	CO92 $pCD1^-$	12
YPA45	CO92 Δ*pla* $pCD1^-$	42
Plasmids		
pLP-PROTet-6×HN	Expression vector that contains $P_{LtetO-1}$ promoter	Clontech
pVM1286	Plasmid containing tetracycline repressor; $Strep^r$	Clontech
pSS	pLP-PROTet-6×HN with DNA containing an RBS, *yadA* signal sequence, HA tag, and SmaI, NheI, and BglII restriction sites inserted between the EcoRI and HindIII restriction sites	This work
pSS::YADA	pSS containing *Y. enterocolitica yadA* lacking native signal sequence	This work
pSS::YAPA	pSS containing *yapA* lacking predicted signal sequence	This work
pSS::YAPE	pSS containing *yapE* lacking predicted signal sequence	This work
pSS::YAPF	pSS containing *yapF* lacking predicted signal sequence	This work
pSS::YAPG	pSS containing *yapG* lacking predicted signal sequence	This work
pSS::YAPJ	pSS containing *yapJ* lacking predicted signal sequence	This work
pSS::YAPK	pSS containing *yapK* lacking predicted signal sequence	This work
pSS::YAPL	pSS containing *yapL* lacking predicted signal sequence	This work
pSS::YAPM	pSS containing *yapM* lacking predicted signal sequence	This work
pMWO-005	Expression vector containing $P_{LtetO-1}$ promoter, P_{N25} *tetR* repressor, pSC101 ori, and multiple cloning site from pWKS130; Kan^r	M. W. Obrist
pMWO-005::HA-YAPA	pMWO-005 containing *yapA* from pSS::YAPA	This work
pMWO-005::HA-YAPE	pMWO-005 containing *yapE* from pSS::YAPE	This work
pMWO-005::HA-YAPF	pMWO-005 containing *yapF* from pSS::YAPF	This work
pMWO-005::HA-YAPG	pMWO-005 containing *yapG* from pSS::YAPG	This work
pMWO-005::HA-YAPJ	pMWO-005 containing *yapJ* from pSS::YAPJ	This work
pMWO-005::HA-YAPK	pMWO-005 containing *yapK* from pSS::YAPK	This work
pMWO-005::HA-YAPL	pMWO-005 containing *yapL* from pSS::YAPL	This work
pMWO-005::HA-YAPM	pMWO-005 containing *yapM* from pSS::YAPM	This work

[a] Strep, streptomycin; RBS, ribosome binding site.

water throughout the experimental course. Infections were preformed as described previously (12, 41). Groups of 10 mice were infected for each time point. Matched groups of five mice were mock infected for each experiment, using sterile PBS administered by the same route of inoculation. At 48 and 72 h postinfection, cervical lymph nodes (following subcutaneous infection) or lungs (following intranasal infection) were harvested and placed in RNALater (Life Technologies) for storage at −80°C or placed directly into TRIzol reagent (Life Technologies) for immediate processing. Once all time points were complete, tissues were mechanically homogenized in TRIzol reagent at a ratio of 5 lungs per 10 ml or 10 lymph nodes per 10 ml.

RNA isolation and qRT-PCR. From homogenized tissues, RNA was extracted with TRIzol reagent by dividing each sample into 1-ml volumes and following the manufacturer's recommended protocol for RNA extraction from tissues. Following RNA extraction, each preparation was treated with DNase I (Life Technologies) at 37°C for 2 h. RNA was precipitated with ethanol and then subjected to a second treatment with DNase I at 37°C for one additional hour. From *Y. pestis* cultures, RNA was extracted and DNase I treated using a RiboPure-Bacteria Kit (Life Technologies) as described by the manufacturer. Using 2 μg of DNase-treated RNA for template, cDNA synthesis was performed with SuperScript III reverse transcriptase (Life Technologies) as specified by the manufacturer. For cDNA synthesis, 500 ng of random hexamer primers was used for broth-derived samples, or 11.6 ng of *Y. pestis* genome-directed primers (The Genome Center, Washington University, St. Louis, MO) was used for tissue-derived samples. Each 25-μl quantitative reverse transcription-PCR (qRT-PCR) mixture contained 0.5 μl of cDNA, 12.5 μl of 2× SYBR green master mix (Qiagen, Valencia, CA), and 0.5 μl each of a pair of 100 μM gene-specific primers (Table 2). Data were normalized to *Y. pestis* CO92 *gyrB* (gyrase B) mRNA, and relative fold change was calculated by using the $\Delta\Delta C_T$ method (where C_T is threshold cycle) (5, 61). DNase I-treated RNA (not subjected to reverse transcription) and uninfected tissues (subjected to reverse transcription) served as controls for DNA contamination and host-specific background amplification. For gene-specific reactions, normalization was performed to *gyrB* reactions run simultaneously (on the same plate), and comparisons to broth-derived samples were made only when run on the same plate as respective tissue-derived samples to control for run-to-run variation.

Operon analysis. Primers were designed to amplify short products internal to the individually annotated genes YPO0606-YPO0608 and YPO0821-YPO0824 as well as the intergenic regions within each of these loci (Table 2). The following PCR templates were used: (i) *Y. pestis* CO92 genomic DNA, (ii) RNA isolated from *Y. pestis* cultured in BHI broth at 26°C, (iii) cDNA prepared from DNase-treated RNA, and (iv) nuclease-free water (Sigma). Following amplification for 30 cycles, PCR products were resolved by standard DNA electrophoresis techniques on a 1% agarose gel.

RESULTS AND DISCUSSION

Identification of autotransporters in *Y. pestis* CO92. Many Gram-negative bacteria encode multiple autotransporters, and preliminary analysis of the *Y. pestis* genomes indicated that this is also the case for *Y. pestis* (33, 72). In an attempt to identify all the putative conventional autotransporters in *Y. pestis* CO92, we used an *in silico* approach to search the available

TABLE 2. Primers used in this work

Primer function and name	Primer sequence (5′–3′)
Constructing pSS	
pSS fwd	GGAATTCAAGGAGATATACATATGACTAAAGATTTTAAGATCAGTGTCTCT
pSS rev	CGAAGCTTAGATCTGCTAGCCCCGGGCTTAGCGTAATCTGGAACATCGTATGGG TAGGCAAATGCATATGGAGATGACAAC
Cloning into pSS	
yadA fwd	TCCCCCGGGAATAATGACGAGGTTCATTTTACAGCA
yadA rev	CCCAAGCTTTTACCACTCGATATTAAATGATGCATTGTACATGAC
yapA fwd	TCCCCCGGGGTGTCACAAATAGCAACCACTGATACAC
yapA rev	CGGGATCCTTAGAAGCTGTAACCCACGTTCAGATTAAT
yapF fwd	TTTTCCCGGGGATCAGACCCTCCACTTCGC
yapF rev	CCCAAGCTTCTAGAACGCCCAGCCCAGAT
yapG fwd	GGCTAGCAACCCGGACCATGAAGGTATC
yapG rev	CGAAGCTTATAGGCACAGGTATCGTTTTATCAATGGATATTA
yapJ fwd	CTAGCTAGCGCATGCACCAGCCCCGG
yapJ rev	CCCAAGCTTGATACCCCGATATAACAAAACCGTCCTGTA
yapK fwd	CTAGCTAGCTGCAATAGCTCGGGGGTGGG
yapK rev	CCCAAGCTTAAAACGATTTACCCGCTAATATAAAACGAT
yapL fwd	TTTTCCCGGGGATTCATGTATTGATTATACTGTCACTGAT
yapL rev	CCCAAGCTTTTAGAAATTAATCCGGAAACCGATATTAGC
yapM fwd	TTTTCCCGGGGTAGTATGCCCACCAGAAGC
yapM rev	CCCAAGCTTTTAGAAGTGTTTAGAAACACTCAGACCGAT
qRT-PCR	
gyrB qRT fwd	TCGCCGTGAAGGTAAAGTTC
gyrB qRT rev	ATTGGTAAAGGTCTGGAAACTTGGCC
yapC qRT fwd	ATGCCGCAATTACTGTCACCAACG
yapC qRT rev	TTAACAATGGTACCCGTCGCCAGA
yapE qRT fwd	AGCCAGTTTGTTGGTGCCTCTTTG
yapE qRT rev	ATACCGCCGAGTGGTTATTAGCCT
yapF qRT fwd	TAAGATCTGGCGTTTATCCGCCGT
yapF qRT rev	TATGATCGCCCGTGTTATGCGGTT
yapG qRT fwd	AACCCGGACCATGAAGGTATCGTT
yapG qRT rev	AGTATTAACGGCCGTATGCTCTGC
yapH qRT fwd	TTTGGCCCTATCTCTGGGCAGTAT
yapH qRT rev	TCTGCCTGCGTGCTGACAGTAATA
yapJ qRT fwd	GGTCTTTTTACCGCAAATGTTCAG
yapJ qRT rev	TTGGTGGTAAAGCAATAGTAGAAA
yapK qRT fwd	CCTATTTCTACCTCACCCGCTCAA
yapK qRT rev	TTTGTGGTAAGACGAGGGTGGAGA
yapL qRT fwd	ACTGCTGGTAGCGAAGATCACCAT
yapL qRT rev	TGGTACCTGAGGCAATTTGAGCAG
yapM qRT fwd	TACTCTCGCCATAAGTATCGCTGC
yapM qRT rev	TGACACAGCCTTGCCATCATTAGC
caf1 qRT fwd	CAGCCAGGATTTCTTTGTTC
caf1 qRT rev	ACGGTTACGGTTACAGCATC
fyuA qRT fwd	GCTTCTCGCATGATAAATCC
fyuA qRT rev	ATATAGCCTGCGGATAGCTG
Operon analysis	
YPO0821 fwd	CACAGTACAAGCCTTCACCAGGTT
YPO0821 rev	TGCGGGATATGAAGAGAGGTTCCA
YPO0822 fwd	TCAGGCAGCACAAGTGAATGCAAC
YPO0822 rev	ACTAAGTTAGACGCGGTGTTCGCT
yapM fwd	CGTGATGCTCAAACAGCCATTCGT
yapM rev	TGTCGTCGTCACCCAAGAATCTGT
YPO0824 fwd	TACACACCTCACCTTTCGGCCAAT
YPO0824 rev	AACCAATGCCTTCGATTTCTCGCC
YPO0821-2 fwd	AGCTATCGATGCTGGAACCTCTCT
YPO0821-2 rev	GCATCAAGGCAGCCATAATTCCCA
YPO0822-3 fwd	CAATGGGTAAAGATGACTCACGGG
YPO0822-3 rev	AGCAGCGATACTTATGGCGAGAGT
YPO0823-4 fwd	CGAAGGCTATATCGGTCTGAGTGT
YPO0823-4 rev	TATTGGCCGAAAGGTGAGGTGTGT
yapF fwd	TAAGATCTGGCGTTTATCCGCCGT
yapF rev	TATAGATACCGCTGGCAAAGGCGT
YPO0606-7 fwd	AGTATCGCTTCGCCAACAGTACCT
YPO0606-7 rev	ATCAGTAAAGCAACAGCAACGGCG
YPO0607 fwd	CCAACCTCGATTTGTTCGGCGTTT
YPO0607 rev	TTTCTGGCGCATCTTTGGCATCAG
YPO0608 fwd	TGACGGTGTTGGTGTCGATGAGAA
YPO0608 rev	CATTGCCCTTGCGATCAACGAAGT
YPO0607-8 fwd	TCGATAGCAGCGGCAAGATCTCAA
YPO0607-8 rev	AATCGTTCACTGTCCGGTCATCGT

TABLE 3. Putative autotransporters in *Y. pestis* CO92

Protein	ORF	Length of protein (aa)	Predicted signal peptide (aa)[a]	Predicted beta domain (aa)	Homolog in *Yersinia* strain:			
					KIM	Microtus	IP32953	8081
YapC	YPO2796	638	1–23	382–622	y1134	YP_1153	YPTB1061	
YapE	YPO3984	1,072	1–34	805–1051	y3845	YP_3347	YPTB3824	YE4059
YapF	YPO0606	761	1–24	481–749	y3573	YP_2924	YPTB3449	
YapG	YPO0587	994	1–49	719–980	y3591	YP_2907	YPTB3471	
YapH	YPO1004	3,705	1–76[b]	3424–3684	y3396	YP_3415	YPTB3303	
YapJ	YPO1672	1,268	1–16; 1–54	989–1244	y1834	YP_1803	—[c]	
YapK	YPO0309	1,269	1–17; 1–55	957–1214	y0567	YP_0465	YPTB0365	
YapL	YPO3028	759	1–28	493–744	y1454	YP_2651	YPTB2746	
YapM	YPO0823	728	1–27	447–716	y3210	YP_2833	YPTB3072	
YapA	YPO2886	1,458[d]	1–28[e]	1194–1443	y1346	YP_2752	YPTB2848	
YapB	YPO2887	1,052	1–28	907–1050[f]	y1345		YPTB2850	
							YPTB2849	
	YPO0765	666		384–654	y3428		YPTB3286	

[a] Signal sequence prediction using SignalP, version 3.0 (8).
[b] Also predicted by Szabady et al. (68).
[c] Unique to *Y. pestis* and paralogous to YPO0309 and YPO0765; also predicted by Derbise et al. (19).
[d] *Y. pestis* Orientalis YapA lacks a signal peptide and is 1,432 aa.
[e] Signal sequence length in *Y. pestis* Medievalis KIM.
[f] Frameshift resulting in a truncation of the β-domain by 123 aa in *Y. pestis*.

genome database for open reading frames with C-terminal regions that contained conserved autotransporter β-domains (Pfam accession number PF03797). This approach yielded 12 ORFs on the *Y. pestis* CO92 chromosome that have putative β-domains (Table 3). The predicted proteins encoded by these ORFs range in size from 638 to 3,705 amino acids (aa) in length. All 12 ORFs are conserved in the *Y. pestis* KIM strain (72; this work), 10 are conserved in the human-avirulent *Y. pestis* Microtus strain (63), and 11 are conserved in *Y. pseudotuberculosis* IP32953 (13). Within this group of genes, there is little similarity outside the predicted β-domains, with the notable exception that *yapJ* and *yapK* share 98% nucleotide identity across 55% of the passenger domain. *yapE* is the only *yap* that has a homolog in *Y. enterocolitica* (42, 69), and only *yapM* appears to have homologs outside the *Yersinia* genus.

Upon identification of these 12 putative autotransporters, we further examined the ORFs to determine the location of a predicted signal peptide, passenger domain, and β-domain of each putative protein. These analyses suggested that three of these ORFs are not functional autotransporters in CO92. YPO0765 contains multiple mutations that result in several frameshifts. *yapB* (YPO2887) contains a conserved frameshift mutation that truncates the β-domain by 123 residues in both *Y. pestis* CO92 and KIM strains and is disrupted by an IS*285* insertion element in Microtus (18, 51, 63), leaving it unlikely to translocate properly across the outer membrane. *Y. pseudotuberculosis* encodes two copies of *yapB*, directly adjacent to each other on the chromosome, and both appear to contain a full-length β-domain (13).

Interestingly, *yapA* (YPO2886) appears to lack a predicted signal sequence in the Orientalis biovar (*Y. pestis* CO92 and IP275 strains). In *Y. pseudotuberculosis* IP32953 and the *Y. pestis* Medievalis and Antiqua biovars, *yapA* contains a predicted 28-residue signal sequence. Analysis of the DNA sequence upstream of YPO2886 in *Y. pestis* CO92 revealed the presence of an in-frame predicted signal sequence similar to the one in the other biovars. Sequence analysis revealed that the Orientalis biovar contains a point mutation (ATG to AGG) in the equivalent predicted Medievalis and Antiqua start codons that would result in an ORF containing a signal sequence. We verified the presence of the point mutation in our laboratory strain of CO92 by sequencing the region surrounding the start codon of YPO2886 (data not shown). These findings indicate that the Medievalis and Antiqua strains have *yapA* genes encoding signal peptides, but the Orientalis biovar likely lacks a functional YapA.

The other nine autotransporters in CO92 appear to contain signal peptides and β-domains that would allow for the proper translocation of each protein. Outside the predicted autotransporter β-domain, the Yaps share little similarity with other characterized proteins or functional domains found in the NCBI conserved domain database (CDD) (47, 48). The CDD lists two subgroups for pertactin-like autotransporter passenger domains, PL1 and PL2. The PL1 group includes the IgA1 proteases of *Neisseria* and *Haemophilus*, serine protease autotransporters of the *Enterobacteriaceae* (SPATEs), and nonprotease autotransporters such as TibA and pertactin. The PL2 group contains exclusively nonprotease autotransporters such as Ag43, AIDA-1, IcsA, and ShdA. Based on their sequences, YapA, YapC, YapE, and YapL are predicted to fall within the PL1 subgroup, and YapG, YapH, YapJ, and YapK fall within the PL2 subgroup; YapF and YapM have no clear assignment to either subgroup. These predictions are based on sequences near the more highly conserved C-terminal ends of these proteins and leave possibly unique, N-terminally located functions largely unpredicted.

While we hypothesize that all of the Yaps described here are conventional autotransporters, Yen et al. previously suggested that YapF and YapM are trimeric autotransporters (72). These two classes of autotransporters have different β-domains, with the trimeric family having a smaller β-domain that requires trimerization for successful translocation (16). The prediction by Yen et al. stemmed from their findings that the β-domains of YapF and YapM share more sequence identity to the β-domain of the trimeric autotransporter YadA than the conventional autotransporter AIDA-1 (72). However, it is well

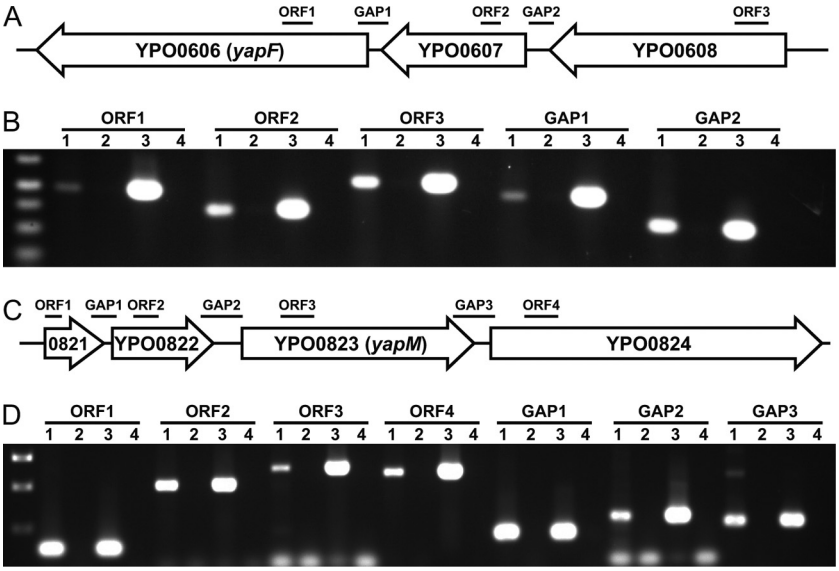

FIG. 1. Operon structure of *yapF* and *yapM*. Map of *yapF* (A) and *yapM* (C) genomic regions in *Y. pestis*. Bars indicate predicted PCR products from internal regions of ORFs or that span the gaps between genes. In the genomic region containing *yapF*, the intergenic region between *yapF* and YPO0607 is 59 bp, and that between YPO0607 and YPO0608 is 101 bp (A). In the genomic region containing *yapM*, the intergenic region between YPO0821 and YPO0822 is 21 bp, that between YPO0822 and YPO0823 is 114 bp, and that between YPO0823 and *yapM* is 69 bp (C). Primers used are listed in Table 2. RT-PCR demonstrates that *yapF* (B) and *yapM* (D) are present in operons. Templates were as follows: lanes 1, RNA; lanes 2, no reverse transcriptase (negative control); lanes 3, DNA (positive control); lanes 4, no template (negative control).

established that autotransporter β-domains do not have high sequence similarity (38). Our conclusion that these two proteins are more likely conventional autotransporters is based on secondary structure analysis. Identification of conserved domains in YapF and YapM with a search of the NCBI CDD revealed that the C-terminal domains of these proteins are more likely to be members of the autotransporter superfamily (referred to as AT-1 by Yen et al.) than the YadA superfamily (referred to as AT-2 by Yen et al.) Furthermore, secondary structure analysis of these proteins with Jpred 3 (15) suggests the presence of an α-helical linker region followed by 12 to 14 extended regions, which is more consistent with a conventional autotransporter β-domain than a trimeric β-domain (α-helix followed by four extended regions) (data not shown). Finally, during our analysis of the localization of the Yaps, we were able to observe multimers of YadA by Western blotting but never observed multimers of any of the Yap proteins (described below). Taken together, we believe that the data suggest that YapF and YapM are more likely to be conventional than trimeric autotransporters.

The majority of these autotransporters (*yapC*, *yapE*, *yapF*, *yapG*, *yapH*, *yapK*, *yapL*, and *yapM*) are retained in the same chromosomal locations with high sequence identity following the divergence of *Y. pseudotuberculosis* and *Y. pestis*. Their retention may imply a function generally useful in infections by both closely related *Yersinia* species while the inactivation of *yapA*, *yapB*, and YPO0765 during the emergence of *Y. pestis* may indicate that these gene products play a role in gastrointestinal disease. Given their various sizes, diversity of sequence, and relative paucity of similarity to proteins of known function, these autotransporters may represent novel adaptations to the environments encountered by *Y. pseudotuberculosis* and *Y. pestis*.

***yapF* and *yapM* are found in operons.** Bacterial genes that are involved in a common biological pathway are often found arranged in operons, where the sequential order and close proximity of genes presumably facilitate their cotranscription and balance the stoichiometry of protein production (37, 74). We previously showed that in *Y. pestis*, *yapE* is cotranscribed with the ORF immediately downstream (42), a finding that prompted us to consider the possibility that other *yap* genes are part of operons. Analysis of the genomic context of each of the *yap* genes indicated that *yapF* (YPO0606) and *yapM* (YPO0823) were present in the same orientation with multiple, closely spaced upstream or downstream genes (Fig. 1A and C). Using RT-PCR, both of these genes were found to be cotranscribed with flanking genes (Fig. 1B and D). Control reaction mixtures lacking template or reverse transcriptase were negative for the presence of DNA contamination. Together, these data indicate that *yapF* is likely to be the third and last gene in an operon containing YPO0608 and YPO0607, which both encode hypothetical proteins (Fig. 1B). *yapM* is likely to be the third gene in an operon of four ORFs including YPO0821, YPO0822, and YPO0824 (Fig. 1D).

While most of the *yap* genes are restricted to known *Y. pestis* and *Y. pseudotuberculosis* strains (*yapE* being the only *yap* with a homolog in *Y. enterocolitica*), *yapM* has homologs outside the *Yersinia* genus in *Salmonella enterica* subspecies *arizonae* (ATCC BAA-731), *Edwardsiella ictaluri* (ATCC 33202), *Edwardsiella tarda* (ATCC 23685), *Proteus mirabilis* (ATCC 29906), and *Proteus penneri* (ATCC 35198). It is noteworthy that the entire putative *yapM*-containing operon appears to be present wherever *yapM* is present, suggesting that *yapM* is part of a functionally linked group of cotranscribed genes. In all instances, *yapM* homologs are followed by a large gene with homology to glycosaminoglycan (GAG) lyases (35, 67), indi-

cating that YapM may contribute to interactions with glycosaminoglycans, an abundant component of extracellular matrix.

Yaps are exported, surface-exposed proteins. While sequence homology suggested the presence of β-domains in the Yap proteins, it needed to be tested experimentally whether or not these regions are capable of mediating translocation of the passenger domains to the outer surface of the bacterium. To monitor the translocation of the Yaps, we designed a plasmid-based expression system that allowed us to easily generate an epitope-tagged version of each Yap. Incorporation of an HA epitope allows monitoring of protein localization by Western blotting with an anti-HA antibody. Thus, we engineered a plasmid to generate a fusion of the *yadA* signal sequence and an HA epitope tag to the amino-terminal region of the passenger domain of each putative autotransporter. The HA tag was placed at the N terminus because previous work suggested that tagging autotransporters on the C-terminal end interferes with the proper function of the β-domain and results in mislocalization of the protein (data not shown; also J. St. Geme III, personal communication) (Fig. 2A). Furthermore, expression of these fusion proteins was controlled with a tetracycline-inducible promoter (29, 73). The region between the predicted signal sequence and the end of each gene (with the exception of the pseudogenes *yapB* and YPO0765 and of *yapH*, which is too large for standard cloning techniques) was amplified by PCR and cloned into the plasmid. The *Y. enterocolitica* autotransporter *yadA* was also cloned into this plasmid and used as a positive control for the system. These plasmids were transformed into *E. coli* DH5αPRO, which contains the tetracycline (Tet) repressor and thus allowed for control of *yap* expression.

To determine if the Yaps are exported, bacteria expressing the tagged proteins were treated with either proteinase K or pronase. Surface-exposed proteins would be accessible to the proteases, resulting in digestion of the HA-tagged portion and loss of signal by Western blotting while intracellular proteins would be protected from proteolysis and remain uncleaved. Surface proteolysis to localize outer surface proteins relies on the bacteria remaining intact throughout the procedure, and, therefore, the proteases do not gain access to intracellular proteins. To ensure that only outer surface proteins were accessible to proteases, we monitored the stability of the periplasmic maltose binding protein (MalE) (55). In cases where we intentionally compromised the integrity of the bacterial cell wall (by sonication, chemical lysis, or heat treatment), MalE was readily digested by both proteases (Fig. 2B). In our localization experiments, however, MalE remained undigested by either protease (Fig. 2C), confirming that intracellular proteins were not accessible to the proteases and that this assay is suitable for detecting surface-exposed proteins.

These surface proteolysis assays demonstrated that HA-tagged YadA, YapE, YapF, YapJ, YapK, YapL, and YapM are exported across the outer membrane of *E. coli* and accessible to the proteases (Fig. 2C). Though we previously showed native YapE to be surface localized and processed (42), this assay confirmed that the presence of an epitope tag and a generic signal sequence do not change the ability of YapE to be translocated or processed. With the exception of YapF and YapM, the proteins were sensitive to both proteases and were completely digested within 30 min. YapM demonstrated a partial resistance to proteinase K cleavage. After 30 min, proteinase K treatment yielded a truncated fragment of YapM that remained associated with the bacteria. When incubation with proteinase K was increased to 1 h, this smaller fragment was further digested, and the HA tag no longer remained associated with the bacteria (data not shown). YapF was more resistant to proteinase K digestion, and the protein remained intact even after 1 h of incubation with the protease (data not shown). Both YapF and YapM, however, were as sensitive to pronase digestion as the other Yaps. Since YapF and YapM previously were suggested to be trimeric autotransporters (72), we tested our tagged constructs for evidence of trimer formation by analyzing unboiled and nondenatured samples of each of these proteins along with a tagged version of YadA (a known trimeric autotransporter). While trimer formation was seen when HA-YadA was left unboiled, no condition showed evidence of YapF or YapM trimers. YapF and YapM consistently migrated near the predicted molecular masses for each monomer, 79.5 kDa and 78.5 kDa, respectively (data not shown).

In addition to the proteins associated with the bacterial surface, three Yap proteins appeared to be released from the surface of *E. coli*. Truncated fragments of HA-tagged YapA, YapE, and YapG were recovered from the culture supernatants following protein production (Fig. 2C and D). During a time course of induction experiment, YapA and YapG were detected in the supernatants within 30 min after aTc treatment, and unprocessed full-length intermediates disappeared from the cell pellet by 120 min. Processing of YapA and YapG in *E. coli* was dependent on the outer surface protease OmpT. Expression of HA-YapA or HA-YapG in the *ompT* mutant UT5600 resulted in the presence of stable full-length proteins on the bacterial surface and absence of detectable proteins in the culture supernatant. Similar results were observed in a DH5αPRO strain with *ompT* deleted, and processing by OmpT consistent with previously published work for native YapE (42) was seen for HA-YapE (data not shown).

Type V secretion is conserved among Gram-negative bacteria, as are the accessory proteins required for secretion by this system. Therefore, we expect that localization of autotransporters in *E. coli* will be highly predictive of the localization of autotransporters in their native species (e.g., *Y. pestis*). However, to confirm this hypothesis, we compared the localization of the Yaps seen in *E. coli* to that seen in *Y. pestis.* Immunofluorescence of intact *Y. pestis* expressing HA-tagged Yaps was performed to detect surface-exposed proteins. As was observed in *E. coli*, YapF, YapJ, YapK, and YapM were all exported and present on the surface of *Y. pestis*, while the three proteins that were predicted to be secreted, YapE, YapG, and YapA, were not readily detected in a wild-type strain, suggesting secretion in *Y. pestis* (Fig. 3A and data not shown). Also in agreement with our *E. coli* data that predicted that cleavage of the secreted proteins is omptin dependent, deletion of the *Y. pestis* omptin Pla resulted in increased signal of YapE, YapG, and YapA on the surface of *Y. pestis* (Fig. 3 and data not shown).

To further demonstrate surface localization of YapF, YapJ, YapK, and YapM, each of these strains was subjected to surface proteolysis, resulting in a decrease or complete loss of fluorescent signal observed for all strains (Fig. 3A). Again, as found in *E. coli*, YapF and YapM demonstrated partial resistance to proteinase K treatment in *Y. pestis* (fluorescence is reduced but not eliminated in these samples). For all of the Yaps, a ring of fluorescence outlined the bacteria, correspond-

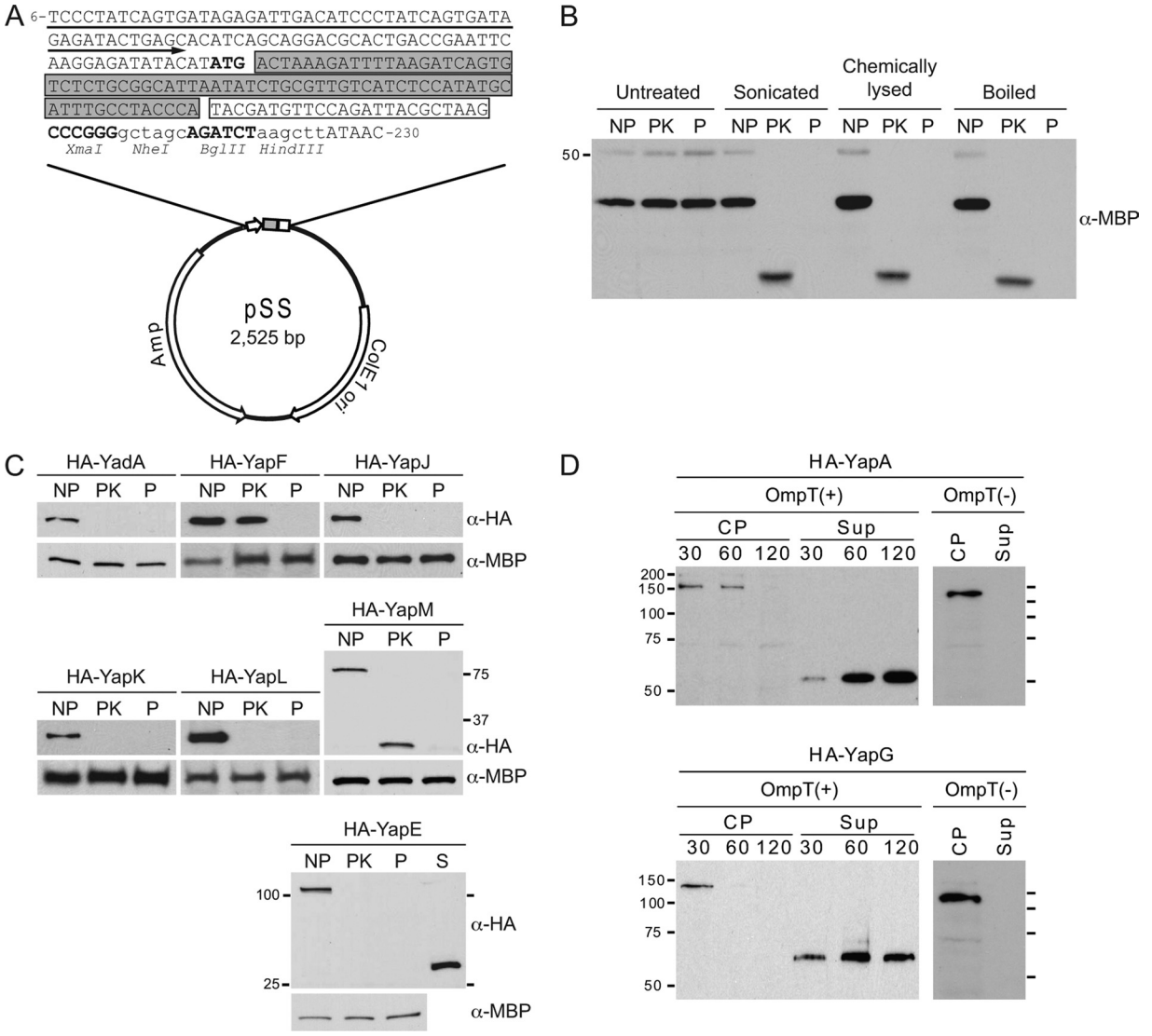

FIG. 2. Localization of the Yaps in *E. coli*. (A) Plasmid pSS was constructed such that each of the *yap* genes could be expressed with the addition of an N-terminal HA epitope tag (white box) and *yadA* signal sequence (gray box) in place of each gene's native predicted signal sequence. Expression of these genes is controlled by the *tetO* operator (underlined with a black arrow). (B) Western blot analysis of *E. coli* cell pellets that were subjected to either mock treatment, sonication, alkaline lysis, or boiling and were subsequently left untreated (no protease [NP]) or treated with proteinase K (PK) or pronase (P). Stability of MalE was determined using anti-maltose binding protein (α-MBP) antibody. (C) Western blot analysis of cell pellets from *E. coli* expressing HA-tagged Yap proteins that were subjected to protease treatment (surface proteolysis). Following growth to exponential phase and protein induction with anhydrous tetracycline (aTc), 2 OD_{600} equivalents of bacterial cells were harvested either prior to protease treatment (NP) or following treatment with proteinase K (PK) or pronase (P) for 30 min. A 0.1-OD_{600} equivalent of each sample was resolved by SDS-PAGE, transferred to polyvinylidene difluoride membrane, and probed with anti-HA (α-HA) or anti-maltose binding protein (α-MBP) antibodies. (D) Western blot analysis of cell pellet (CP) and supernatant (Sup) from *E. coli* cultures expressing HA-tagged YapA or YapG. Samples were harvested from an *E. coli* $OmpT^+$ strain (DH5αPRO) at 30, 60, or 120 min postinduction or an *E. coli* $OmpT^-$ strain (UT5600) at 120 min postinduction. Samples were resolved and probed as described for panel B. Molecular mass markers are indicated on either side of the Western blots.

ing to the periphery of visually intact bacteria when the image was overlaid on a simultaneously obtained DIC image.

To confirm that the samples used for immunofluorescence represented intact bacteria, samples also were analyzed by Western blotting with an anti-HA antibody and anti-MalE antibody as described for *E. coli*. Where signal was seen by immunofluorescence, intact protein was observed by Western blotting, and protease treatment eliminated anti-HA signal while leaving MalE intact (Fig. 3B). Furthermore, preparation of supernatants confirmed secretion of YapE, YapG, and YapA in *Y. pestis* that is dependent on the omptin Pla (Fig. 3B and data not shown). While HA-YapL levels were too low to detect by immunofluorescence, extended developing times during Western analysis confirmed surface localization of this protein in *Y. pestis* (Fig. 3B).

While our results demonstrated that pilot studies in *E. coli* can serve as useful tools to predict localization of autotransporters from other bacteria, we did observe slight differences in *Y. pestis*. In *E. coli*, secreted YapG was predominantly found as a single peptide. However, in *Y. pestis*,

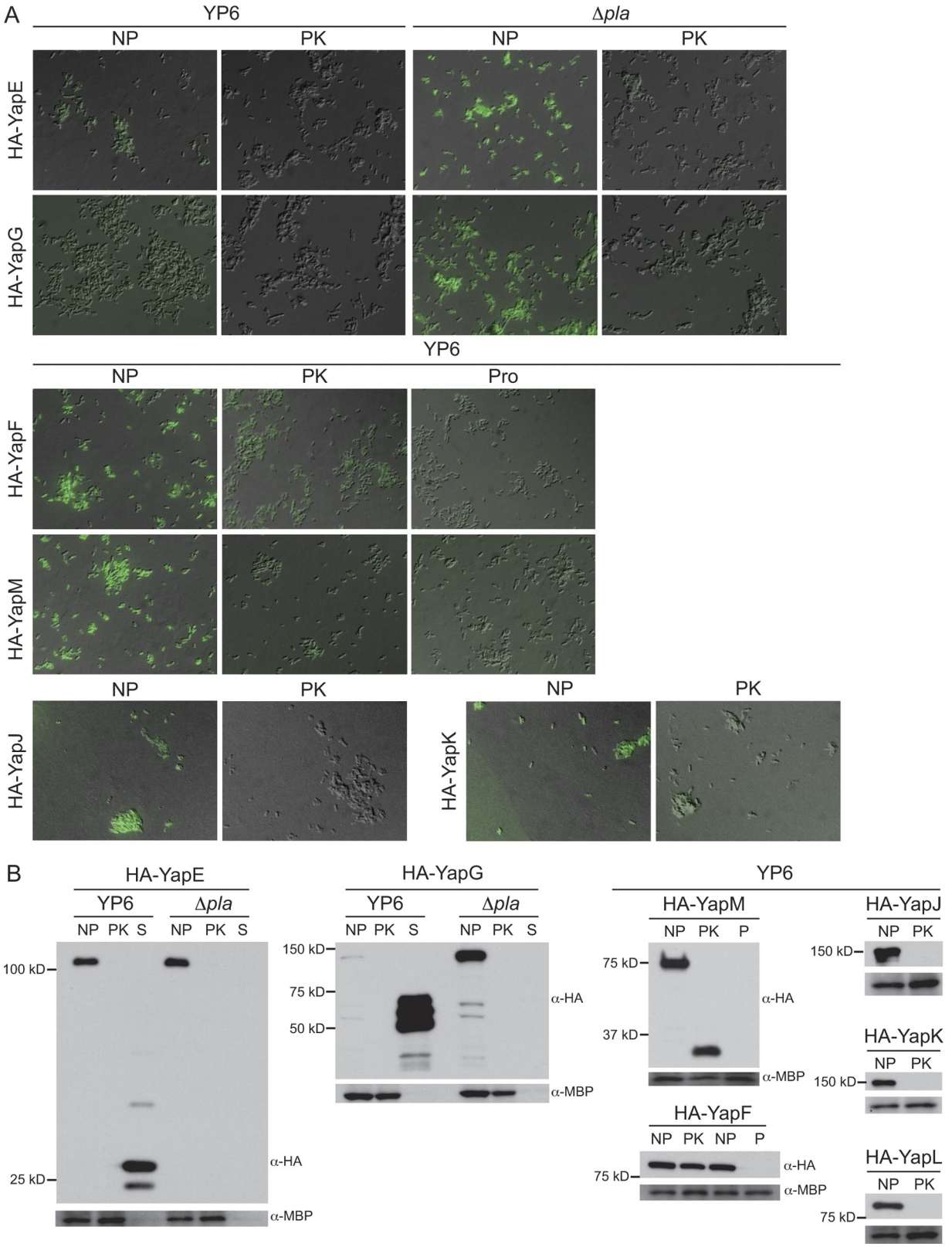

FIG. 3. Localization of the Yaps in *Y. pestis*. (A) Determination of surface exposure of Yaps in *Y. pestis* by immunofluorescence microscopy. FITC (fluorescence) and differential interference contrast (DIC) micrograph overlays were created of YP6 or isogenic Δ*pla* strains expressing HA-tagged Yap proteins that were subjected to protease treatment (surface proteolysis), as described in the legend of Fig. 2. Samples of each strain were either given no protease (NP), treated with proteinase K (PK), or treated with pronase (P) (only YapF and YapM), after which 10 μl was fixed on a poly-D-lysine-coated coverslip and stained with a 1:500 dilution of Alexa Fluor 488-conjugated monoclonal mouse anti-hemagglutinin IgG. (B) Western blot analysis of cell pellets (NP, PK, and P) and supernatants (S) from the samples used in panel A. For each sample, a 0.1-OD_{600} equivalent was resolved by SDS-PAGE, transferred to polyvinylidene difluoride membrane, probed with anti-HA (α-HA), and then stripped and reprobed with anti-maltose binding protein (α-MBP) antibodies. Molecular mass markers are indicated on either side of Western blots.

TABLE 4. Expression of *caf1* and *yap* genes compared to *gyrB* expression

Gene	ΔC_T ($C_{T\ \text{target}} - C_{T\ gyrB}$) at[a]:	
	26°C	37°C
caf1	3.6 ± 0.6	−5.7 ± 0.7
yapC	2.8 ± 0.4	3.7 ± 0.3
yapE	6.2 ± 0.6	6.0 ± 0.7
yapF	2.6 ± 0.8	2.5 ± 0.5
yapG	3.7 ± 0.2	4.1 ± 0.6
yapH	7.1 ± 0.5	7.9 ± 0.8
yapJ	4.5 ± 0.7	3.5 ± 0.4
yapK	6.3 ± 0.9	6.0 ± 0.6
yapL	4.9 ± 0.7	4.4 ± 1.0
yapM	3.9 ± 1.2	3.9 ± 1.1

[a] Data represent the mean ± standard deviation from three independent experiments for liquid cultures of YP6 grown in BHI medium supplemented with 2.5 mM $CaCl_2$.

we observed the presence of at least three peptides in the supernatant. Previous work has indicated that Pla is a more promiscuous and efficient protease than OmpT (30), suggesting that this is the reason for multiple peptides in the *Y. pestis* supernatant. The resulting peptides are very similar in size, and it is unclear how the additional processing by Pla may impact function of YapG. These data, together with previous work (24, 42, 72), verify that the predicted β-domains of YapA, YapC, YapE, YapF, YapG, YapJ, YapK, YapL, and YapM are capable of mediating translocation of their respective passenger domains across the bacterial outer membrane, confirming that these proteins fit the description of autotransporters. Furthermore, using Yap-specific antibodies, we were able to confirm that native YapE, YapF, YapG, YapJ, YapK and YapM have the same localization patterns as HA-tagged proteins (42; also data not shown), demonstrating that the pSS plasmid is a reliable system to quickly determine the localization of putative autotransporters, that the position of the HA tag does not interfere with localization, and that the native signal sequences of these proteins are functional.

***yap* transcription is induced during mammalian infection.** While Yen et al. demonstrated that *yapA*, *yapC*, *yapE*, *yapF*, *yapG*, *yapH*, *yapL*, and *yapM* are transcribed during *in vitro* growth, their analysis was not quantitative (72). We observed by Western blotting that native YapE, YapG, and YapC expression levels in *Y. pestis* appear to be very low during *in vitro* growth (M. B. Lawrenz, M. C. Lane, and V. L. Miller, unpublished data). To determine if all of the Yaps are similarly expressed at low levels, we compared the relative levels of each *yap* transcript to a known *Y. pestis* virulence factor, the *caf1* gene, which is also expressed at low levels during *in vitro* growth at 26°C. As a point of reference, we used the constitutively expressed gene *gyrB*, which is often used to normalize bacterial numbers in qRT-PCR (12, 60). At 26°C, *caf1* transcription is at basal levels, and detection of transcript occurred 3.6 cycles later than for *gyrB* (ΔC_T). Transcript levels of all of the *yap* genes were also lower than the level of *gyrB* at 26°C and detectable at 2.6 to 7.1 cycles later than the *gyrB* transcript (Table 4). Based on these C_T values, our data suggest that *yapC*, *yapF*, *yapG*, *yapJ*, and *yapM* transcript levels are comparable to *caf1* transcription under these noninducing conditions. *yapE*, *yapH*, *yapK*, and *yapL* transcription appears to be even lower, with C_T values 1.3 to 3.5 cycles later than transcription of *caf1*. These results demonstrate that the *yap*s are transcribed at very low levels during standard *in vitro* growth conditions.

Many autotransporters are virulence factors and, therefore, needed during mammalian infection. We hypothesized that if the *yap* genes contribute to virulence in the mammalian host, then expression levels may be low during *in vitro* growth but induced during infection. To determine the expression profiles of the *yap* genes within the host, we utilized the C57BL/6J mouse models of both bubonic and pneumonic plague (12, 41). Transcript levels at 48 and 72 h postinfection during either subcutaneous (bubonic) infection (in cervical lymph nodes) or during intranasal (pneumonic) infection (in lungs) were determined for each of the *yap* genes by qRT-PCR. Transcript levels under each condition were normalized to the housekeeping gene *gyrB* before being compared to the similarly normalized transcript levels found in *Y. pestis* cultures grown in BHI broth.

Following subcutaneous infection, all of the *yap* genes were induced by 48 h in the cervical lymph node, relative to broth culture, and elevated levels were maintained through 72 h postinfection. Transcript levels for *yapC*, *yapE*, *yapF*, *yapG*, *yapK*, and *yapM* were up between 2- and 6.5-fold, and levels for *yapH*, *yapJ*, and *yapL* were elevated over 10-fold by 48 h (Fig. 4A). Transcript levels of *yapC*, *yapF*, *yapG*, and *yapM* were up between 4.6- and 8.2-fold by 72 h, while levels for *yapH*, *yapE*, *yapJ*, and *yapK* were elevated over 15-fold. *yapE* and *yapK* showed the largest change in expression over the course of

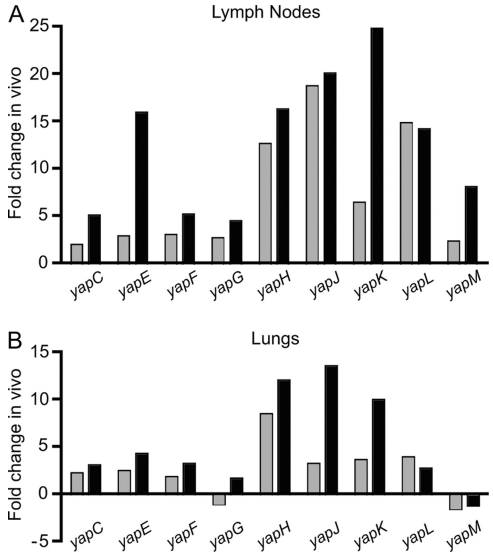

FIG. 4. *yap* expression during bubonic and pneumonic infection. Bars represent the fold change in the level of each transcript in the cervical lymph nodes or lungs at 48 h (gray) or 72 h (black) postinfection compared to the level of that same transcript in a 26°C broth culture. Quantitative RT-PCRs using gene-specific primers were performed in triplicate using cDNA template from infected tissue samples of 10 mice per time point for each infection route and on cDNA from a 26°C broth-grown culture. Fold change was calculated by the $\Delta\Delta C_T$ method by first normalizing *in vivo* transcript levels to the level of the housekeeping gene *gyrB* and then comparing those to similarly normalized transcript levels from a 26°C broth culture. The error present in triplicate technical replicates of all samples was less than 2.9% percent for *gyrB* and 6.1% for the *yap* genes.

TABLE 5. Effect of growth conditions on *yap* expression

Gene	Fold change in gene expression under the indicated condition(s)[a]								
	37°C[b]	2.5 mM $CaCl_2$		2,2′-dipyridyl[c]		Acidic pH (6.0)[d]		Alkaline pH (8.0)[d]	
		26°C	37°C	26°C	37°C	26°C	37°C	26°C	37°C
yapC	NC	NC	NC	NC	NC	NC	NC	NC	NC
yapE	NC	NC	NC	NC	NC	NC	NC	NC	NC
yapF	2.7 ± 1.6	NC	NC	NC	NC	NC	NC	NC	NC
yapG	NC	NC	NC	NC	NC	−2.5 ± 1.1	NC	−2.5 ± 1.3	NC
yapH	NC	NC	NC	NC	NC	NC	NC	3.5 ± 1.7	NC
yapJ	3.4 ± 1.5	NC	NC	NC	NC	NC	NC	NC	NC
yapK	3.0 ± 1.2	NC	−2.7 ± 1.2	NC	NC	NC	NC	NC	NC
yapL	2.9 ± 1.1	NC	NC	NC	NC	NC	NC	NC	NC
yapM	2.0 ± 0.1	2.6 ± 1.1	NC	−3.1 ± 1.0	−4.3 ± 2.5	NC	−4.2 ± 0.1	NC	NC
caf1	605.5 ± 106.1								

[a] Data represent the mean ± standard deviation in fold change ($\Delta\Delta C_T$) from three independent experiments. NC, no change ($2 > X > -2$).
[b] Relative to growth at 26°C.
[c] Data are for a 60-min treatment, relative to untreated BHI broth.
[d] Relative to medium buffered to maintain pH 7.0.

infection, with *yapE* up 5.4-fold and *yapK* up 3.9-fold at 72 h compared to 48 h. We similarly observed an increase in transcription of most of the genes in the lungs during pneumonic infection (Fig. 4B). However, transcript levels were not as elevated in the lungs as observed in the lymph nodes. In addition, transcript levels of *yapG* and *yapM* did not appear to change in the lungs compared to levels in broth culture. As observed in the lymph nodes, *yapH* was the most highly induced gene in the lungs. Interestingly, *yapL* transcript decreased at the 72-h time point in both tissues, suggesting that YapL levels decrease over the course of either infection route. These results from two different routes of infection indicate that *yap* expression is generally increased during mammalian infection compared to *in vitro* growth and suggest that these proteins contribute to mammalian infection.

***yap* genes show limited responsiveness to known virulence factor-inducing conditions *in vitro*.** In order to better understand what stimuli may be responsible for changes in *yap* expression *in vivo*, several *in vitro* conditions that are known to influence the expression of virulence factors in *Y. pestis*, namely, temperature, calcium, iron, and pH, were examined. The shift from the ambient temperature of the flea vector (~26°C) to the body temperature of a warm-blooded mammalian host (~37°C) is a major cue for increased expression of many virulence factors in *Y. pestis* (65). While microarray analysis has largely confirmed previously identified temperature-induced genes, including the Ysc-Yop type III secretion system, F1 capsule, pH 6 antigen, and hemin storage system (31), low levels of *yap* expression in culture may put these genes below the threshold of detection by microarray. When *yap* expression was analyzed by qRT-PCR, we found that *yapF*, *yapJ*, *yapK*, *yapL*, and *yapM* were all induced 2-fold or greater at 37°C compared to expression at 26°C (Table 5). By comparison, the *caf1* gene, a known temperature-regulated gene, is induced 600-fold upon the shift to 37°C (Table 5). While this response to host temperature is similar to the increase seen for *yapF*, *yapJ*, *yapK*, and *yapL* in early pneumonic infection (48 h), it accounts for only a fraction of the increases seen at later times or in bubonic infection, suggesting that temperature is not solely responsible for the *in vivo* changes in *yap* transcription.

Expression of the type III secretion system genes and export of the Yops are intimately tied both to growth of *Y. pestis* at 37°C and levels of available calcium (64). Therefore, the addition of $CaCl_2$ to the medium was evaluated. Only two genes responded to Ca^{2+} levels. *yapM* was induced in response to calcium during growth at 26°C, and *yapK* was repressed in the presence of calcium at 37°C (Table 5). Again, most *yap* genes showed no change in expression levels, and the subtle changes in *yapK* and *yapM* do not explain the large changes in transcription *in vivo*.

During infection, bacterial pathogens encounter a severely iron-limited environment, a condition known to induce the coordinate regulation of virulence factors that assist bacteria in obtaining host-derived iron (reviewed in reference 45). *Y. pestis* has several methods to circumvent iron limitation, including the production of multiple siderophores and iron import systems responsive to iron limitation (28, 53, 75). Sequence analysis of the promoter regions (−500 to −1 bp) upstream of each *yap* gene did not reveal any evidence of even the minimal recognition unit for binding of the ferric uptake repressor (Fur) (7). This suggests that these genes are unlikely to be positively regulated by low-iron conditions but does not exclude the possibility of regulation by iron concentration. The *yap* genes were investigated for responsiveness to low-iron conditions by treating growth medium with the iron chelator 2,2′-dipyridyl (75). qRT-PCR analysis of the *fyuA* gene, a known iron-responsive gene (28, 75), was performed to confirm that these conditions produced the expected response. Following 30 min of 2,2′-dipyridyl treatment at 26°C or 37°C, *fyuA* was induced 7.7- and 11.3-fold, respectively, over untreated conditions (data not shown). *yapM* was the only gene found to be responsive to low-iron conditions, where it was repressed at both 26°C and 37°C (Table 5). *yapM* is the only *yap* not induced in the lungs at either time point and is induced to only a low level at 48 h in the lymph nodes. This pattern of relative gene expression may suggest investigation of the role of this gene outside the mammalian host, such as in coloniza-

tion of the flea vector, where *Y. pestis* grows at cooler temperatures and thrives on the iron-rich blood meal (39).

Changes in pH have been shown to regulate the expression of autotransporters in other bacteria (2, 32), and *Y. pestis* is known to alter the expression of virulence genes in a pH-dependent manner (44). During normal growth of *Y. pestis* CO92 pCD1$^-$ in BHI broth, the pH drops from ~7.5 to ~6.5 over the course of 8 h. However, specific pH levels can be maintained by the addition of appropriate buffers to the medium. Under acidic conditions (pH 6.0), none of the *yap* genes was induced, and only *yapG* was repressed more than 2-fold (Table 5). Under alkaline conditions (pH 8.0), *yapG* was repressed 2.5-fold at 26°C (Table 5), suggesting that the ideal conditions for *yapG* expression are within a narrow range around neutral pH. The only gene found to be induced more than 2-fold in response to pH was *yapH*, which was induced 3.5-fold at pH 8.0 and 26°C (Table 5).

While the *yap* genes were responsive to the environment of the host, these genes were not dramatically impacted by any of the *in vitro* conditions tested, including temperature. Within the host, *Y. pestis* almost certainly processes numerous simultaneous signals that allow the bacterium to fine-tune gene expression. Our data indicate that, while some of these specific conditions may be contributing factors for induction of the *yap* genes during infection, there are likely numerous individual and combinatorial cues that remain unexplored.

Concluding remarks. Numerous autotransporters have been characterized as factors important for pathogenic interactions of bacteria with their respective hosts, and the same may be true for the autotransporters of *Y. pestis*. Bioinformatic analyses presented here and elsewhere predicted 12 type V proteins in *Y. pestis* strain CO92 (Orientalis biovar), of which we predicted 9 would be functional, and 12 type V proteins predicted for strain KIM5 (Medievalis biovar), of which 10 would be predicted to be functional. Given that the passenger domains of these Yaps exhibit little similarity to known autotransporters, these proteins may have novel activities and interact with previously uncharacterized host targets and pathways.

The localization of native YapC and YapE in *E. coli* and *Y. pestis* has been previously published (24, 42), and here we determined the localization of seven additional *Yersinia* autotransporters. YapC, YapF, YapJ, YapK, YapL, and YapM were all found to be localized to the surface of the bacterium and accessible to exogenously added protease (demonstrated in both *E. coli* and *Y. pestis*) or exogenously added antibody (demonstrated in *Y. pestis*) (24; this work). Furthermore, YapA, YapG, and YapE were shown to be transported to the cell surface and then released in an omptin-dependent manner (42; this work). Together these data demonstrate that all the putative Yaps of *Y. pestis*, with the exception of YapH, which has not been tested, behave in the expected manner for a type V secreted protein. Future work can now focus on understanding the function of these proteins and their contribution to virulence.

Our localization data are an important advance on the initial report by Yen et al. (72). In their study, the authors primarily concentrated on five putative autotransporters from KIM5, including 4 of the 10 conventional autotransporters we discuss here. Our data confirm their preliminary work for YapA and YapC, extend their YapK findings to show that it is a surface-exposed protein, and demonstrate localization of the other Yaps. However, our results did differ on the localization of YapG. Yen et al. reported that YapG is a membrane-bound protein (72), and we clearly demonstrate that this protein is cleaved and secreted into the supernatant. One possibility for these differences could be that two point mutations inadvertently introduced in the construct used by Yen et al. interfered with the proper secretion of the protein. Alternatively, and more likely, YapG secretion may previously have been missed because the authors' strategy to localize the proteins (silver stain analysis of total membrane proteins) was not specific enough to correctly identify YapG. Our use of an HA tag and specific antibodies allowed us to eliminate signal from other proteins that may have led to misinterpretation of the data by Yen et al. (72). Regardless of the reason, we have confirmed with YapG-specific antibodies that native YapG is rapidly secreted in *Y. pestis* in the same manner as the HA-tagged version.

The *yap* genes are not significantly expressed under standard laboratory growth conditions or induced by temperature shift to 37°C. Thus, it is noteworthy that all the *yap* genes show some increase in expression during mammalian infection, and some of the *yap* genes show quite large changes in expression. Localization of the Yaps to the cell surface combined with increased expression during infection is consistent with a role for these proteins during infection. Differences in relative transcript levels observed between the lymph nodes and lungs may indicate that specific Yaps contribute to different stages of disease. For example, *yapE* transcription is considerably higher in the lymph nodes than in the lungs, suggesting a more important role for YapE in bubonic infection as opposed to pneumonic infection. Supporting this hypothesis, a *yapE* mutant is attenuated in lymph node colonization but has a much less significant impact on pneumonic colonization (42). *yapJ* and *yapK*, the most similar of the *yap* genes, show different expression patterns in the lymph nodes, suggesting a divergence in function for two genes that are closely related. Finally, *yapH* was the most highly upregulated gene in either infection model, but the role of *yapH* during infection is unclear. Previous work from Styer et al. identified *yapH* in a transposon screen for virulence determinants in a *Caenorhabditis elegans* model of *Y. pestis* infection (66). Future animal studies with *yap* mutants will clarify the role of these autotransporters in *Y. pestis* infection.

ACKNOWLEDGMENTS

We thank Roger Pechous for advice on the isolation of RNA from mouse tissues, Wyndham Lathem and Lauren Bellows for preliminary data on gene expression *in vivo*, and Kimberly Walker for critical editing of the manuscript. *Y. pestis* genome-directed primers were generously provided by William E. Goldman. The UT5600 strain was a gift from Scott Hultgren. We thank Markus Obrist for use of pMWO-005 prior to publication.

This study was supported by funds from National Institutes of Health grants R56AI078930 (V.L.M.), R01AI64313 (V.L.M.), and U54AI057157 (Southeast Regional Center for Biodefense and Emerging Infectious Diseases, subproject 4.1, to V.L.M.), a Morse/Berg Fellowship from the Department of Molecular Microbiology, Washington University (J.D.L.), a Ruth L. Kirschstein National Research Service Award (AI085923) (M.C.L.), and the Biomedical Research Apprenticeship Program (BioMedRAP), Washington University (D.G.C.).

REFERENCES

1. **Achtman, M., et al.** 1999. *Yersinia pestis*, the cause of plague, is a recently emerged clone of *Yersinia pseudotuberculosis*. Proc. Natl. Acad. Sci. U. S. A. **96:**14043–14048.
2. **Alamuri, P., and H. L. Mobley.** 2008. A novel autotransporter of uropathogenic *Proteus mirabilis* is both a cytotoxin and an agglutinin. Mol. Microbiol. **68:**997–1017.
3. **Altschul, S. F., W. Gish, W. Miller, E. W. Myers, and D. J. Lipman.** 1990. Basic local alignment search tool. J. Mol. Biol. **215:**403–410.
4. **Andrews, G. P., et al.** 2010. Identification of in vivo-induced conserved sequences from *Yersinia pestis* during experimental plague infection in the rabbit. Vector Borne Zoonotic Dis. **10:**749–756.
5. **Applied Biosystems.** 1997. User bulletin no. 2: ABI Prism 7700 sequence detection system. Applied Biosystems, Foster City, CA.
6. **Ari, T. B., et al.** 2010. Interannual variability of human plague occurrence in the Western United States explained by tropical and North Pacific Ocean climate variability. Am. J. Trop. Med. Hyg. **83:**624–632.
7. **Baichoo, N., and J. D. Helmann.** 2002. Recognition of DNA by Fur: a reinterpretation of the Fur box consensus sequence. J. Bacteriol. **184:**5826–5832.
8. **Bendtsen, J. D., H. Nielsen, G. von Heijne, and S. Brunak.** 2004. Improved prediction of signal peptides: SignalP 3.0. J. Mol. Biol. **340:**783–795.
9. **Benz, I., and M. A. Schmidt.** 2011. Structures and functions of autotransporter proteins in microbial pathogens. Int. J. Med. Microbiol. **301:**461–468.
10. **Bertherat, E., et al.** 2007. Plague reappearance in Algeria after 50 years, 2003. Emerg. Infect. Dis. **13:**1459–1462.
11. **Bodelon, G., E. Marin, and L. A. Fernandez.** 2009. Role of periplasmic chaperones and BamA (YaeT/Omp85) in folding and secretion of intimin from enteropathogenic *Escherichia coli* strains. J. Bacteriol. **191:**5169–5179.
12. **Cathelyn, J. S., S. D. Crosby, W. W. Lathem, W. E. Goldman, and V. L. Miller.** 2006. RovA, a global regulator of *Yersinia pestis*, specifically required for bubonic plague. Proc. Natl. Acad. Sci. U. S. A. **103:**13514–13519.
13. **Chain, P. S., et al.** 2004. Insights into the evolution of *Yersinia pestis* through whole-genome comparison with *Yersinia pseudotuberculosis*. Proc. Natl. Acad. Sci. U. S. A. **101:**13826–13831.
14. **Chain, P. S., et al.** 2006. Complete genome sequence of *Yersinia pestis* strains Antiqua and Nepal516: evidence of gene reduction in an emerging pathogen. J. Bacteriol. **188:**4453–4463.
15. **Cole, C., J. D. Barber, and G. J. Barton.** 2008. The Jpred 3 secondary structure prediction server. Nucleic Acids Res. **36:**W197–201.
16. **Cotter, S. E., N. K. Surana, and J. W. St Geme III.** 2005. Trimeric autotransporters: a distinct subfamily of autotransporter proteins. Trends Microbiol. **13:**199–205.
17. **Cully, J. F., Jr, T. L. Johnson, S. K. Collinge, and C. Ray.** 2010. Disease limits populations: plague and black-tailed prairie dogs. Vector Borne Zoonotic Dis. **10:**7–15.
18. **Deng, W., et al.** 2002. Genome sequence of *Yersinia pestis* KIM. J. Bacteriol. **184:**4601–4611.
19. **Derbise, A., et al.** 2010. Delineation and analysis of chromosomal regions specifying *Yersinia pestis*. Infect. Immun. **78:**3930–3941.
20. **Doll, J. M., et al.** 1994. Cat-transmitted fatal pneumonic plague in a person who traveled from Colorado to Arizona. Am. J. Trop. Med. Hyg. **51:**109–114.
21. **Eisen, R. J., et al.** 2006. Early-phase transmission of *Yersinia pestis* by unblocked fleas as a mechanism explaining rapidly spreading plague epizootics. Proc. Natl. Acad. Sci. U. S. A. **103:**15380–15385.
22. **Eisen, R. J., et al.** 2008. Persistence of *Yersinia pestis* in soil under natural conditions. Emerging Infect. Dis. **14:**941–943.
23. **Falgarone, G., H. S. Blanchard, F. Virecoulon, M. Simonet, and M. Breban.** 1999. Coordinate involvement of invasin and Yop proteins in a *Yersinia pseudotuberculosis*-specific class I-restricted cytotoxic T cell-mediated response. J. Immunol. **162:**2875–2883.
24. **Felek, S., M. B. Lawrenz, and E. S. Krukonis.** 2008. The *Yersinia pestis* autotransporter YapC mediates host cell binding, autoaggregation and biofilm formation. Microbiology **154:**1802–1812.
25. **Finn, R. D., et al.** 2006. Pfam: clans, web tools and services. Nucleic Acids Res. **34:**D247–251.
26. **Finn, R. D., et al.** 2010. The Pfam protein families database. Nucleic Acids Res. **38:**D211–222.
27. **Flashner, Y., et al.** 2004. Generation of *Yersinia pestis* attenuated strains by signature-tagged mutagenesis in search of novel vaccine candidates. Infect. Immun. **72:**908–915.
28. **Gao, H., et al.** 2008. The iron-responsive Fur regulon in *Yersinia pestis*. J. Bacteriol. **190:**3063–3075.
29. **Gossen, M., and H. Bujard.** 1993. Anhydrotetracycline, a novel effector for tetracycline controlled gene expression systems in eukaryotic cells. Nucleic Acids Res. **21:**4411–4412.
30. **Haiko, J., M. Suomalainen, T. Ojala, K. Lahteenmaki, and T. K. Korhonen.** 2009. Invited review: breaking barriers—attack on innate immune defences by omptin surface proteases of enterobacterial pathogens. Innate Immun. **15:**67–80.
31. **Han, Y., et al.** 2004. Microarray analysis of temperature-induced transcriptome of *Yersinia pestis*. Microbiol. Immunol. **48:**791–805.
32. **Henderson, I. R., J. Czeczulin, C. Eslava, F. Noriega, and J. P. Nataro.** 1999. Characterization of Pic, a secreted protease of *Shigella flexneri* and enteroaggregative *Escherichia coli*. Infect. Immun. **67:**5587–5596.
33. **Henderson, I. R., F. Navarro-Garcia, and J. P. Nataro.** 1998. The great escape: structure and function of the autotransporter proteins. Trends Microbiol. **6:**370–378.
34. **Hinchliffe, S. J., et al.** 2003. Application of DNA microarrays to study the evolutionary genomics of *Yersinia pestis* and *Yersinia pseudotuberculosis*. Genome Res. **13:**2018–2029.
35. **Huang, W., et al.** 2003. Crystal structure of *Proteus vulgaris* chondroitin sulfate ABC lyase I at 1.9Å resolution. J. Mol. Biol. **328:**623–634.
36. **Isberg, R. R., D. L. Voorhis, and S. Falkow.** 1987. Identification of invasin: a protein that allows enteric bacteria to penetrate cultured mammalian cells. Cell **50:**769–778.
37. **Jacob, F., and J. Monod.** 1961. Genetic regulatory mechanisms in the synthesis of proteins. J. Mol. Biol. **3:**318–356.
38. **Jacob-Dubuisson, F., R. Fernandez, and L. Coutte.** 2004. Protein secretion through autotransporter and two-partner pathways. Biochim. Biophys. Acta **1694:**235–257.
39. **Jarrett, C. O., et al.** 2004. Transmission of *Yersinia pestis* from an infectious biofilm in the flea vector. J. Infect. Dis. **190:**783–792.
40. **Jong, W. S., et al.** 2010. YidC is involved in the biogenesis of the secreted autotransporter hemoglobin protease. J. Biol. Chem. **285:**39682–39690.
41. **Lathem, W. W., S. D. Crosby, V. L. Miller, and W. E. Goldman.** 2005. Progression of primary pneumonic plague: a mouse model of infection, pathology, and bacterial transcriptional activity. Proc. Natl. Acad. Sci. U. S. A. **102:**17786–17791.
42. **Lawrenz, M. B., J. D. Lenz, and V. L. Miller.** 2009. A novel autotransporter adhesin is required for efficient colonization during bubonic plague. Infect. Immun. **77:**317–326.
43. **Li, B., et al.** 2009. High-throughput identification of new protective antigens from a *Yersinia pestis* live vaccine by enzyme-linked immunospot assay. Infect. Immun. **77:**4356–4361.
44. **Lindler, L. E., M. S. Klempner, and S. C. Straley.** 1990. *Yersinia pestis* pH 6 antigen: genetic, biochemical, and virulence characterization of a protein involved in the pathogenesis of bubonic plague. Infect. Immun. **58:**2569–2577.
45. **Litwin, C. M., and S. B. Calderwood.** 1993. Role of iron in regulation of virulence genes. Clin. Microbiol. Rev. **6:**137–149.
46. **Lorange, E. A., B. L. Race, F. Sebbane, and B. J. Hinnebusch.** 2005. Poor vector competence of fleas and the evolution of hypervirulence in *Yersinia pestis.* J. Infect. Dis. **191:**1907–1912.
47. **Marchler-Bauer, A., et al.** 2009. CDD: specific functional annotation with the Conserved Domain Database. Nucleic Acids Res. **37:**D205–210.
48. **Marchler-Bauer, A., and S. H. Bryant.** 2004. CD-Search: protein domain annotations on the fly. Nucleic Acids Res. **32:**W327–331.
49. **Matchett, M. R., D. E. Biggins, V. Carlson, B. Powell, and T. Rocke.** 2010. Enzootic plague reduces black-footed ferret (*Mustela nigripes*) survival in Montana. Vector Borne Zoonotic Dis. **10:**27–35.
50. **Miller, V. L., and J. J. Mekalanos.** 1988. A novel suicide vector and its use in construction of insertion mutations: osmoregulation of outer membrane proteins and virulence determinants in *Vibrio cholerae* requires *toxR*. J. Bacteriol. **170:**2575–2583.
51. **Parkhill, J., et al.** 2001. Genome sequence of *Yersinia pestis*, the causative agent of plague. Nature **413:**523–527.
52. **Pepe, J. C., and V. L. Miller.** 1993. *Yersinia enterocolitica* invasin: a primary role in the initiation of infection. Proc. Natl. Acad. Sci. U. S. A. **90:**6473–6477.
53. **Perry, R. D., P. B. Balbo, H. A. Jones, J. D. Fetherston, and E. DeMoll.** 1999. Yersiniabactin from *Yersinia pestis*: biochemical characterization of the siderophore and its role in iron transport and regulation. Microbiology **145:** 1181–1190.
54. **Perry, R. D., and J. D. Fetherston.** 1997. *Yersinia pestis*: etiologic agent of plague. Clin. Microbiol. Rev. **10:**35–66.
55. **Rasmussen, B. A., V. A. Bankaitis, and P. J. Bassford, Jr.** 1984. Export and processing of MalE-LacZ hybrid proteins in *Escherichia coli*. J. Bacteriol. **160:**612–617.
56. **Rosqvist, R., A. Forsberg, M. Rimpilainen, T. Bergman, and H. Wolf-Watz.** 1990. The cytotoxic protein YopE of *Yersinia* obstructs the primary host defence. Mol. Microbiol. **4:**657–667.
57. **Ruiz-Perez, F., et al.** 2009. Roles of periplasmic chaperone proteins in the biogenesis of serine protease autotransporters of *Enterobacteriaceae*. J. Bacteriol. **191:**6571–6583.
58. **Ruiz-Perez, F., I. R. Henderson, and J. P. Nataro.** 2010. Interaction of FkpA, a peptidyl-prolyl cis/trans isomerase with EspP autotransporter protein. Gut Microbes **1:**339–344.
59. **Sauri, A., et al.** 2009. The Bam (Omp85) complex is involved in secretion of the autotransporter haemoglobin protease. Microbiology **155:**3982–3991.
60. **Schiano, C. A., L. E. Bellows, and W. W. Lathem.** 2010. The small RNA

chaperone Hfq is required for the virulence of *Yersinia pseudotuberculosis*. Infect. Immun. **78:**2034–2044.
61. **Sheets, A. J., and J. W. St Geme III.** 2011. Adhesive activity of the *Haemophilus* cryptic genospecies Cha autotransporter is modulated by variation in tandem peptide repeats. J. Bacteriol. **193:**329–339.
62. **Skurnik, M., Y. el Tahir, M. Saarinen, S. Jalkanen, and P. Toivanen.** 1994. YadA mediates specific binding of enteropathogenic *Yersinia enterocolitica* to human intestinal submucosa. Infect. Immun. **62:**1252–1261.
63. **Song, Y., et al.** 2004. Complete genome sequence of *Yersinia pestis* strain 91001, an isolate avirulent to humans. DNA Res. **11:**179–197.
64. **Straley, S., and W. Bowmer.** 1986. Virulence genes regulated at the transcriptional level by Ca^{2+} in *Yersinia pestis* include structural genes for outer membrane proteins. Infect. Immun. **51:**445–454.
65. **Straley, S. C., and R. D. Perry.** 1995. Environmental modulation of gene expression and pathogenesis in *Yersinia*. Trends Microbiol. **3:**310–317.
66. **Styer, K. L., et al.** 2005. *Yersinia pestis* kills *Caenorhabditis elegans* by a biofilm-independent process that involves novel virulence factors. EMBO Rep. **6:**992–997.
67. **Sutherland, I. W.** 1995. Polysaccharide lyases. FEMS Microbiol. Rev. **16:** 323–347.
68. **Szabady, R. L., J. H. Peterson, K. M. Skillman, and H. D. Bernstein.** 2005. An unusual signal peptide facilitates late steps in the biogenesis of a bacterial autotransporter. Proc. Natl. Acad. Sci. U. S. A. **102:**221–226.
69. **Thomson, N. R., et al.** 2006. The complete genome sequence and comparative genome analysis of the high pathogenicity *Yersinia enterocolitica* strain 8081. PLoS Genet. **2:**e206.
70. **Tong, Z., et al.** 2005. Pseudogene accumulation might promote the adaptive microevolution of *Yersinia pestis*. J. Med. Microbiol. **54:**259–268.
71. **Vadyvaloo, V., C. Jarrett, D. E. Sturdevant, F. Sebbane, and B. J. Hinnebusch.** 2010. Transit through the flea vector induces a pretransmission innate immunity resistance phenotype in *Yersinia pestis*. PLoS Pathog. **6:**e1000783.
72. **Yen, Y. T., A. Karkal, M. Bhattacharya, R. C. Fernandez, and C. Stathopoulos.** 2007. Identification and characterization of autotransporter proteins of *Yersinia pestis* KIM. Mol. Membr. Biol. **24:**28–40.
73. **Yin, D. X., L. Zhu, and R. T. Schimke.** 1996. Tetracycline-controlled gene expression system achieves high-level and quantitative control of gene expression. Anal. Biochem. **235:**195–201.
74. **Yin, Y., H. Zhang, V. Olman, and Y. Xu.** 2010. Genomic arrangement of bacterial operons is constrained by biological pathways encoded in the genome. Proc. Natl. Acad. Sci. U. S. A. **107:**6310–6315.
75. **Zhou, D., et al.** 2006. Global analysis of iron assimilation and *fur* regulation in *Yersinia pestis*. FEMS Microbiol. Lett. **258:**9–17.